



**HAL**  
open science

## Micromegas for Imaging Calorimetry

M. Chefdeville

► **To cite this version:**

M. Chefdeville. Micromegas for Imaging Calorimetry. XVth International Conference on Calorimetry in High Energy Physics CALOR 2012, Jun 2012, Santa Fe, United States. in2p3-00748574

**HAL Id: in2p3-00748574**

**<https://hal.in2p3.fr/in2p3-00748574>**

Submitted on 5 Nov 2012

**HAL** is a multi-disciplinary open access archive for the deposit and dissemination of scientific research documents, whether they are published or not. The documents may come from teaching and research institutions in France or abroad, or from public or private research centers.

L'archive ouverte pluridisciplinaire **HAL**, est destinée au dépôt et à la diffusion de documents scientifiques de niveau recherche, publiés ou non, émanant des établissements d'enseignement et de recherche français ou étrangers, des laboratoires publics ou privés.

# Micromegas for imaging calorimetry

Maximilien Chefdeville on behalf of the LAPP/LC group

LAPP, Université de Savoie, CNRS/IN2P3, Annecy-le-Vieux, France

E-mail: [chefdevi@lapp.in2p3.fr](mailto:chefdevi@lapp.in2p3.fr)

**Abstract.** Gaseous detectors have been used in sampling calorimeters for several years and still remain an attractive option for future collider experiments. The use of Micromegas chambers as active elements of a hadronic calorimeter was proposed a few years ago and stirred up exciting developments of this technology. Basic building blocks of large size chambers acting as signal generating and processing units have been designed and fabricated. They were used to construct two chambers of 1 m<sup>2</sup> size which after test in muon and pion beams, showed excellent performance. The most important results are presented followed by a discussion of the prospects towards realistic calorimeter modules at a future collider experiment.

## 1. Introduction

### 1.1. Calorimetry at a future linear collider

The detailed study of electroweak symmetry breaking and of the properties of a hypothetical standard model Higgs boson are some of the physics goals motivating the construction of a linear electron collider. The physics case is now enhanced with the discovery at LHC of a Higgs-like new particle. At ILC or CLIC [1, 2], several interesting physics channels will appear in multi-jet final states, often accompanied by charged leptons and missing transverse energy. The di-jet energy resolution should be such that  $Z$  and  $W$  bosons can be identified with an accuracy comparable to their natural decay width. This translates into a jet energy resolution of 3–4% over the whole energy range. The approaches followed to meet this requirement are the *Dual Readout* and the *Particle Flow*, respectively studied by the DREAM and CALICE collaborations [3, 4]. The first one is a powerful compensation technique that combines measurements of cherenkov and scintillation light produced by showering particles [5]. On the other hand, the CALICE collaboration develops calorimeters with high 3D imaging capability to identify the jet's charged and neutrals components. Thanks to the granularity, the dominant charged component can be measured very precisely with the tracking system resulting in improved jet energy resolution [6].

### 1.2. Micromegas for calorimetry

Several calorimeter technologies are studied by the CALICE groups such as silicon, scintillators and gas detectors for the active parts with tungsten or steel absorbers. Three HCAL projects presented at this conference are documented in the proceedings: the scintillator analog HCAL and the Glass Resistive Plate Chamber (GRPC) and Micromegas semi-digital HCAL (or SDHCAL). Micromegas is a fast, position sensitive Micro Pattern Gas Detector (MPGD [7]) operating in the proportional mode [8]. Essentially free of space charge effects and thus high rate capable, it suffers very little from aging because it functions in simple gas mixtures (*e.g.* Ar/CO<sub>2</sub>) and at relatively low electric fields and voltages (< 500 V).

## 2. The 1 m<sup>2</sup> Micromegas chamber

### 2.1. Micromegas principle

Micromegas is a parallel plate detector that uses a thin micro-mesh to separate the gas volume into two regions of low and high field. Electrons liberated in the low field region drift towards the mesh and are multiplied in the high field region, inducing a signal with a fast electron component ( $\sim 1$  ns) and an ion tail ( $\sim 150$  ns). The signal is proportional to the gas gain, itself controlled by the mesh voltage. The fast ion collection at the mesh makes Micromegas free of space charge effects which is useful to obtain some information on cell occupancy (semi-digital calorimetry).

### 2.2. Active Sensor Unit

The basic building block of a 1 m<sup>2</sup> chamber is a  $32 \times 48$  cm<sup>2</sup> 8 layer Printed Circuit Board (PCB) dubbed Active Sensor Unit (or ASU). One PCB side consists of the mesh laminated on an anode matrix of 1536 pads of 1 cm<sup>2</sup> at a 128  $\mu$ m distance. The pad's readout is performed by 24 ASICs located on the backside. Passive components are also present on this side to provide protection against gas discharges. The ASICs are read out with 2 Detector Interface boards (DIF, inter-DIF) which distribute voltage to ASICs and mesh. The ASUs can be chained through flexible connectors which allows to read out several of them with one pair of DIF/inter-DIF board.

The 64 channel ASIC, called MICROROC, was developed by LAPP/LC and LAL/Omega groups [9]. Its input stage consists of a diode network for discharge protection, a low noise charge preamplifier (1500 ENC) and 2 shapers of variable peaking time (75–200 ns) and different gains. Shaper signals are compared to 3 thresholds and the result is stored in a 127-event depth memory. Thresholds are common to the 64 channels but individual pedestals can be adjusted with respect to the low threshold. This feature allows to minimize the detector non-uniformity. The ASIC is synchronised to the 5 MHz DIF clock for time-stamping with a 200 ns precision.

### 2.3. Chamber design

The 1 m<sup>2</sup> chamber consists of 6 ASUs assembled in a one gas volume (Fig. 1). Small spacers (1 mm wide, 3 mm high) are inserted between ASUs and support the cathode cover, defining precisely the drift gap. Plastic frames are closing the chamber sides, leaving openings for 2 gas pipes and flexible cables. The chamber is eventually equipped with readout boards and a patch panel for voltage distribution. The total chamber thickness amounts to 9 mm which includes 2 mm for the cathode cover, 3 mm of drift gap and 4 mm for PCB and ASICs. With this mechanical design, we achieve less than 2% of inactive area.

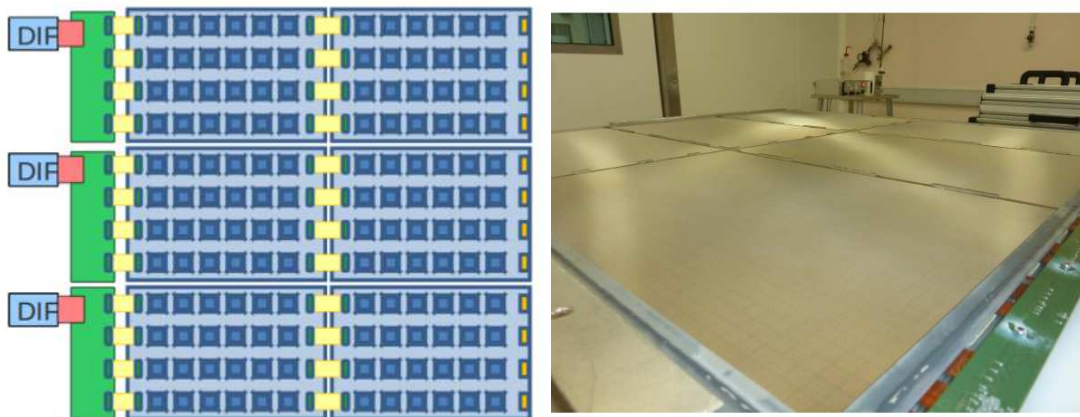


**Figure 1.** Drawing and photograph of the ASIC and mesh sides of the 1 m<sup>2</sup> chamber.

### 3. Chamber response to minimum ionising particles

The response to minimum ionising particles (MIPs) was studied in a 150 GeV/c muon beam at CERN/SPS. The 1 m<sup>2</sup> chamber was flushed with a non-flammable mixture of Ar/CF<sub>4</sub>/iC<sub>4</sub>H<sub>10</sub> 95/3/2. The mesh voltages were varied between 300–420 V (gas gain of 100–8000) and the drift field set to 300 V/cm at the local maximum of the drift velocity. A telescope of small chambers [12] with a point resolution of  $\sim 3$  mm was used to measure efficiency and hit multiplicity at various positions. A trigger signal was provided by a set of 3 scintillators and photomultiplier tubes to discriminate between cosmic background and beam particles.

#### 3.1. Noise and channel occupancy

The noise rate over all channels is equalised to a target value of 0.1 Hz by tuning pedestals and thresholds. This is done with HV set to zero in order to avoid bias from cosmic or beam particles, and is achieved by masking 16 / 9216 channels only. When HV is applied, particles crossing the chamber gas dominate the channel occupancy. Cosmic muons are responsible for a uniform background above which the beam profile clearly separates (Fig. 2 (left)). Using time information (time of trigger and time of hits), the background is removed, leaving a very clean pattern of the beam (see presentation slides).

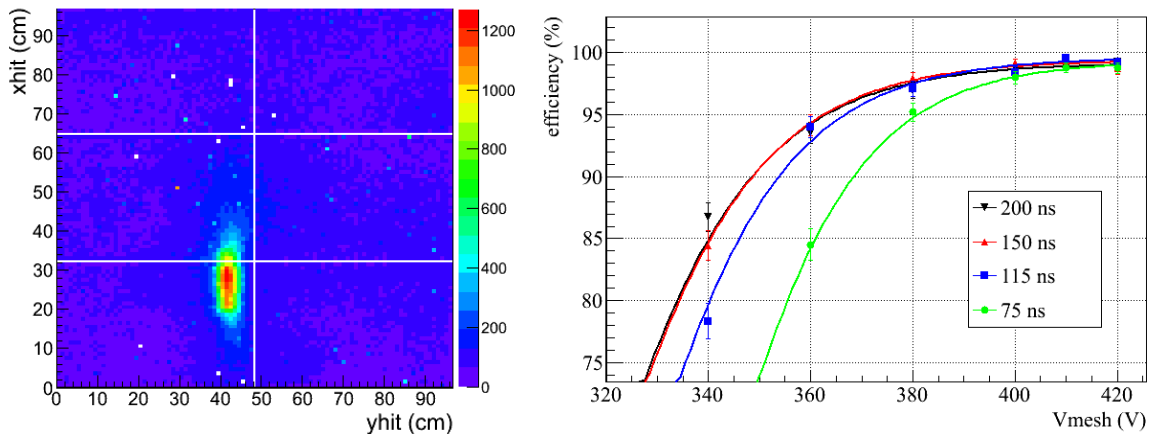


**Figure 2.** Profile of a muon beam crossing the 1 m<sup>2</sup> chamber before applying a cut on the trigger time (left). Efficiency versus mesh voltage curves for various peaking times (right).

#### 3.2. Efficiency study

Beam muons (150 GeV/c) are a good approximation of MIPs which liberate in the drift region a most probable number of 14 electrons. These are multiplied in the amplification region by factors up to  $10^4$  depending on the mesh voltage. The strong dependence of the detection efficiency on the applied voltage is shown in Fig. 2 (right) for voltages of 340–420 V and peaking times of 75–200 ns. The curves indicate that Micromegas signals last between 115–150 ns, as expected for a 128  $\mu$ m gap. For peaking times larger than 150 ns, a gas gain as low as  $10^3$  ( $V_{\text{mesh}} = 365$  V) is sufficient to detect MIPs with an efficiency larger than 95%. This is due to very low readout thresholds of 1–2 fC achieved with the MICROROC chip. Upon full exposure of two chambers, detailed efficiency maps over  $8 \times 8$  cm<sup>2</sup> regions were produced revealing an efficiency of  $(96 \pm 2)$ %. Such a little variation indicates a good control of the chamber dimensions (gas gaps) as well as of the electronics parameters (gains, thresholds).

### 3.3. Multiplicity study

A benefit of Micromegas w.r.t. other gas detector technologies is the limited spatial extension of the avalanche signals. This is a result of the little diffusion experienced by the electrons in the gas. The electrons liberated in the drift gap arrive at the mesh with a transverse spread of  $110\ \mu\text{m}$  RMS [10]. Moreover, electrons liberated by one avalanche are distributed at the anode with a  $20\text{--}30\ \mu\text{m}$  spread [10]. It is thus likely that all electrons from a crossing particle are collected on one pad. As showed in the presentation slides, the hit multiplicity is below 1.15 up to  $390\ \text{V}$  (*i.e.* gain  $G = 3000$ ). At higher gains, neighbouring pads become sensitive to single electrons, increasing the multiplicity to 1.35 at  $420\ \text{V}$  (*i.e.*  $G = 8000$ ). There is however no reason to work in that regime as high MIP efficiency is reached at lower gains (95% at  $G = 1000$ ).

## 4. Chamber response to hadron showers

Measurements in a muon beam allow to define the benchmark performance of the chamber. The various particles generated in a hadron shower, however, are mostly far more ionising than MIPs. The particle density is of course larger, especially in the shower core and where  $\pi^0$  induced electromagnetic showers develop. Larger  $dE/dx$  and multiplicity significantly increase the discharge probability. It is thus mandatory to investigate the response and stability of the chamber in such an environment. Two experimental setups were used.

- (i) The first is the one described in the previous section with an additional  $20\ \text{cm}$  long ( $\sim 1\ \lambda_{\text{int}}$ ) and  $10 \times 10\ \text{cm}^2$  area Fe block placed  $50\ \text{cm}$  upstream of the Micromegas chamber.
- (ii) The second setup is a 50 layer sampling GRPC/Fe calorimeter in which 2 Micromegas chambers were inserted at layer 48 and 49 (*i.e.* behind  $\sim 5\ \lambda_{\text{int}}$  of Fe).

In both cases, a pion beam was used with an energy of  $150\ \text{GeV}$  and  $60\text{--}180\ \text{GeV}$  respectively.

### 4.1. Gas gain study

The average pad signal in a hadron shower is larger than the one induced by a MIP. It can hence be expected that the gas gain necessary to image 95% of the shower is lower than that necessary to detect a MIP with the same efficiency. Using experimental setup (i), the distribution of the number of hits in the chamber was measured at various mesh voltages. A statistics of  $50 \times 10^3$  events was recorded at  $325\ \text{V}$ ,  $350\ \text{V}$  and  $375\ \text{V}$  which translates into gas gains of about 350, 800 and 1700. The number of hit distributions, shown in Fig. 3, exhibit a peak at  $N_{\text{hit}} = 1$  and a long tail from penetrating and showering pions respectively. The distributions at  $350\ \text{V}$  and  $375\ \text{V}$  yield different efficiency to penetrating pions but remarkably, have both a similar tail. It can thus be concluded that a gas gain as low as 800 is sufficient to image most of the shower.

### 4.2. Beam energy study

Compensation is difficult to achieve in sampling hadron calorimeters which are thus non linear devices [11]. With a digital readout, saturation effects add to the complexity of the response. Additional thresholds can probably be used to mitigate saturation effects but the feasibility of this technique still needs to be demonstrated. While this will be the goal of future beam tests, a first measurement of the response of a Micromegas chamber to pions has been carried out with the calorimetric setup (ii). At pion energies from  $60$  to  $180\ \text{GeV}$ , the distribution of hits passing the three thresholds after  $5\ \lambda$  of Fe was measured at  $390\ \text{V}$ . The mean value for the low threshold is plotted versus beam energy in Fig. 3. Because most of the shower particles have been stopped at this depth of the calorimeter, the mean values are small: *e.g.* 5.5 hits et  $100\ \text{GeV}$ . This presumably explains the linear trend, which is also observed for medium and high thresholds. Fortunately, more measurements at various depths should become available by the end 2012 so the linearity of a Micromegas SDHCAL can be assessed.

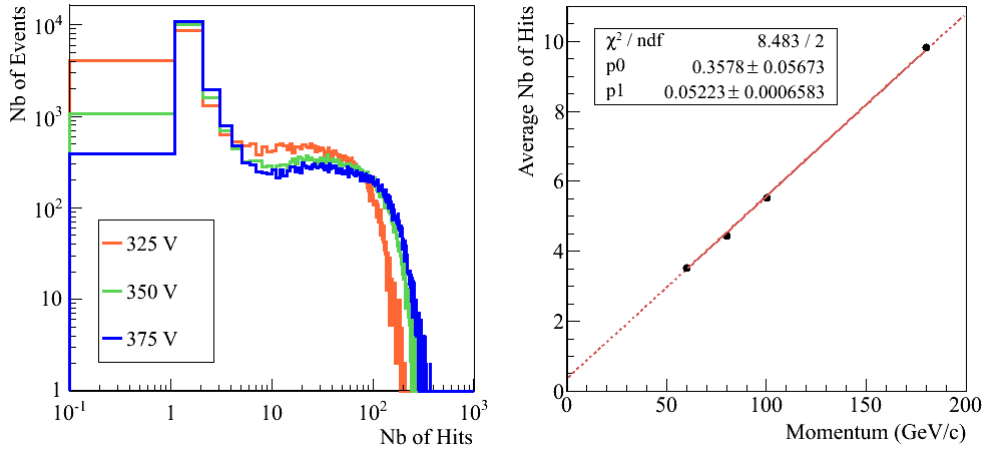


**Figure 3.** Hit distribution from 150 GeV/c pions at various mesh voltages measured with setup (i) (left). Mean value versus pion momentum measured with setup (ii) at 390 V (right).

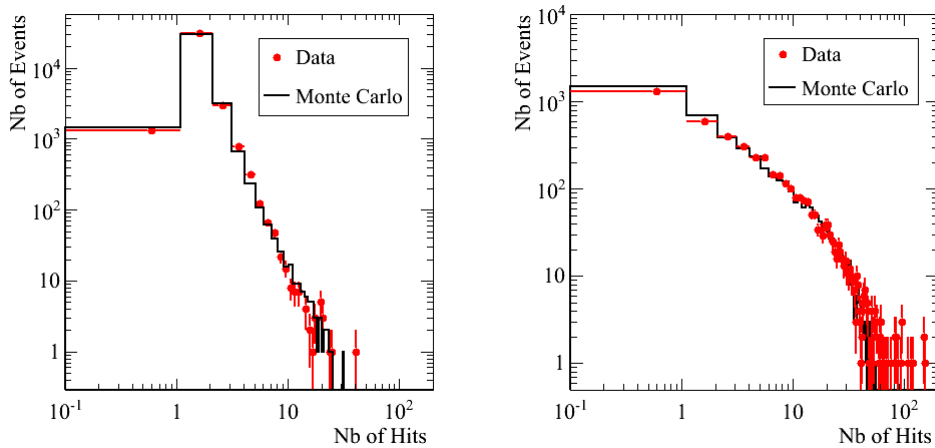


**Figure 4.** Hit distribution from 100 GeV muons (left) and pions (right) as measured at layer 48 of a hadron calorimeter (setup (ii)). Data points are compared to Monte Carlo predictions from GEANT4 LHEP physics list. The mesh voltage was 390 V during both runs.

#### 4.3. Monte Carlo simulation

Computer programs can be used to simulate the development of showers and therefore predict the response of a full Micromegas calorimeter. As a first step in this direction, the number of hit distribution of a single chamber at a given depth of the calorimeter was simulated and compared to test beam data collected with setup (ii). Doing so, a straightforward digitisation procedure was implemented where simulated energy deposits are turned into a number of electrons which diffuse, multiply and are compared to a threshold. A preliminary result of our analysis is presented in Fig.4 (right) which shows the distribution after  $5 \lambda_{\text{int}}$  of Fe for 100 GeV pions. The readout threshold was tuned so as to reproduce the efficiency to muons (Fig.4 (left)). A satisfactory agreement is obtained, both for muons and pions. It should be stressed that no noise was introduced in the simulation, meaning that data are essentially free of noise.

## 5. Prospects towards a technological module

### 5.1. Scalability to large area

The design of the 1 m<sup>2</sup> chamber is scalable in both transverse directions. It is now such that 2 ASUs are chained (forming a slab) but that can in principle be extended to 6 along a total length of 3 m. The current design consists of 3 slabs, each one read out by a pair of DIF/inter-DIF boards. The number of slab can be extended as well.

### 5.2. Chamber thickness and spark protection

At a future linear collider, the calorimetric system will fit inside the magnet. To minimize the solenoid radius and cost, the chamber should be as thin as possible. The Micromegas chamber is 9 mm thick, including the 2 mm thick steel cover. At an ILC, the HCAL absorbers will be made out of steel so the effective chamber thickness is actually 7 mm, already matching the baseline value.

Ways to reduce the thickness further are nevertheless considered. One is to shrink the 3 mm gas gap to 2 mm. This would yield a signal loss that can be compensated by a 50 % increase in gas gain. Another way is to slim the PCB components by adopting thinner ASIC packages and by removing/embedding the protection networks. These supplement MICROROC diodes and may not be mandatory for operation at low gas gains. Also, they could be replaced by a thin resistive layer deposited onto the anode plane. Both options are currently under investigation.

### 5.3. Pressure and temperature effects

Previous studies [12] showed that the gas gain sensitivity to  $P/T$  variations is small ( $-0.5\%/mbar$  and  $1\%/K$  with a slight gas mixture dependence), so the detector response is slightly affected by  $P/T$  variations. The MIP efficiency variation under usual atmospheric changes is negligible, provided that the readout threshold is low enough (*e.g.* 1–2 fC). With additional thresholds at higher values,  $P/T$  changes should probably be corrected for. An on-line solution is to monitor  $P/T$  and adjust the voltage according to the known sensitivity of  $\sim 3\%/V$ .

## 6. Conclusion

Micromegas is a relatively new technology which is studied for calorimetry for the first time. In view of this application, an innovative design of Micromegas detector has been proposed and used to construct two chambers of 1 m<sup>2</sup>. Experimental results on the chamber performance to MIPs are excellent: an efficiency larger than 95 % is achieved while keeping the pad multiplicity below 1.15. The chamber shows a stable behaviour in pion showers and a quantitative understanding of the data is well underway. Although two chambers are insufficient to measure the energy resolution of a  $5 \lambda_{\text{int}}$  Micromegas calorimeter, a test program with four chambers has been established to measure linearity and leakage inside the CALICE Fe structure at the end of 2012.

## References

- [1] ILC Reference Design Report, 2007, ([http://arxiv.org/PS\\_cache/arxiv/pdf/0709/0709.1893v1.pdf](http://arxiv.org/PS_cache/arxiv/pdf/0709/0709.1893v1.pdf)).
- [2] CLIC Conceptual Design Report, 2011, (<https://edms.cern.ch/document/1177771>).
- [3] The RD52 experiment web-page: <http://highenergy.phys.ttu.edu/dream>.
- [4] The CALICE collaboration web-page: <https://twiki.cern.ch/twiki/bin/view/CALICE>.
- [5] R. Wigmans, *Nucl. Instr. and Meth.* **A617** (2010) 129133.
- [6] M.A. Thomson et al., *Nucl. Instr. and Meth.* **A611** (2009) 25-40.
- [7] The RD51 collaboration web-page: <http://rd51-public.web.cern.ch/rd51-public/>.
- [8] Y. Giomataris et al., *Nucl. Instr. and Meth.* **A376** (1996) 29-35.
- [9] C. Adloff et al., *JINST* **7** (2012) C01029.
- [10] S.F. Biagi, *Nucl. Instr. and Meth.* **A421** (1999) 234240.
- [11] R. Wigmans, Calorimetry, *Scientifica Acta* **2**, No. 1, (2008) 18-55.
- [12] C. Adloff et al., *JINST* **4** (2009) P11023.